

The Finnish Research Programme on Nuclear
Power Plant Safety 2015 – 2018,
SAFIR2018SAFIR
Energiforsk AB
Swedish Radiation Safety Authority

Simulation and calibration of rubber materials for seals

Abstract

Finite element (FE) simulations of how rubber materials for seals behave over time is performed. The application is seals for nuclear power plants where seals are exposed to elevated levels of ionizing radiation and temperature.

A major challenge for the simulations is to find an appropriate material model for the rubber materials and how to calibrate it to experiments. Here is a material model proposed that can include effects like creep, permanent set, and temperature dependence. Calibration of material models for relaxation tests on EPDM rubber is performed and presented with good results. Further modelling to include more effects in the material and to simulate leak and tightness of seals are proposed.

RISE Research Institutes of Sweden AB

Postal address
Box 24036
SE-400 22
GÖTEBORG
Sweden

Office location
Gibraltargatan 35
SE-412 79
GÖTEBORG

Phone / Fax / E-mail
+46 10 516 50 00
+46 33 13 55 02
info@ri.se

This document may not be reproduced other than in full,
except with the prior written approval of RISE.

Contents

Abstract.....	1
Contents	2
1 Introduction.....	3
2 Modelling.....	4
2.1 Constitutive modelling.....	4
2.2 Calibration and optimization.....	6
2.2.1 Optimization methods	6
2.2.2 Test data	7
2.3 Simulation	7
2.3.1 Relaxation	8
2.3.2 Compressive set	9
2.3.3 Leak and tightness.....	9
3 Results.....	10
4 Conclusions and further work	14
5 Acknowledgements	15
6 References.....	16

1 Introduction

This report is about simulation of seals in nuclear power plants. The seals are typically made of a rubber material e.g. EPDM and have the form of o-rings. An issue with rubber materials is their creep behavior i.e. they deform over time and can also retain a permanent deformation – permanent set. This can reduce the sealing function since the compressive force on the seal reduces which can cause penetration of the pressurized fluid to be contained by the seal. A further complication in nuclear power applications is elevated temperatures and radiation levels which can accelerate or initiate degradation like creep in polymers like rubbers.

The simulation is performed with finite element (FE) modelling. The advantage of FE modelling is that complex geometry and material behavior can be handled. In this case the complicated behavior of rubber becomes the major difficulty to address here.

The purpose of the project this work is part of is to evaluate how materials for seals degrade in a nuclear power plant environment and how to measure this degradation. The particular aim of this report is the development of simulation methods that can be used to evaluate test methods of aged seal and how they perform in service i.e. provide leak tightness. Further information on the project and testing is available in [1].

2 Modelling

2.1 Constitutive modelling

Rubber is a material that compared to most other engineering materials can undergo extreme deformation and after loading (nearly) go back to the undeformed shape. This property makes rubber suitable for seals e.g. o-rings when assembled in a joint. This is because the rubber material is heavily deformed compared to the surrounding materials e.g. steel which causes it to maintain the sealing pressure if the joint deforms i.e. displacements between the components that are joined. This type of large deformation is modelled with hyper-elasticity which is a generalization of regular elasticity (Hooke's law) that is only valid for small strains. Rubber also exhibits other behaviors like creep and permanent set. For further reading refer to e.g. [2].

The constitutive theory of hyper-elasticity is based on an energy density potential from which the relation between strain and stress is derived. The use of an energy potential leads to that the deformation is reversible causing the material to go back to the original shape (a property of elasticity). Many choices of energy potentials exist that can be used to model rubber, e.g. Neo-Hookean, Mooney-Rivlin, Arruda-Boyce, Ogden, and Yeoh.

An o-ring in a normal application is subjected to compressive strain of moderate magnitude (stretch 0.5 or engineering strain -50 %). In such conditions where the strains are compressive together with moderate shear strains, the Neo-Hookean type material is fully adequate [3], [4] and is here chosen for the elastic part of the material modelling. The more advanced hyper-elastic models are more suitable and needed for cases with large tensile strains where the polymer molecular chains get heavily stretched.

The Neo-Hookean energy potential is the most simple and is

$$\phi = C_{10}(J^{-2/3}I_1 - 3) + \frac{1}{D_1}(J - 1)^2 \quad (1)$$

where $I_1 = \lambda_1^2 + \lambda_2^2 + \lambda_3^2$ is the first invariant, $J = \lambda_1\lambda_2\lambda_3$ is the volume ratio and λ_i are principal stretches. It can be regarded as an extension of the linear elastic material model (Hooke's generalized law) and is valid for large strains. Like the linear elastic model, it has only two material parameters: C_{10} and D_1 that governs elasticity similarly as Young's modulus E and the bulk modulus respectively in linear elasticity. In linear elasticity one often defines the behavior with the parameter Poisson's ratio ν which relates to the compressibility. In the small strain limit, hyper-elastic material models approach the linear elastic behavior where expressions for E and μ can be formed. For the Neo-Hookean model the relations are

$$C_{10} = \frac{E}{4(1 + \nu)} \quad (2)$$

$$D_1 = \frac{6(1 - 2\nu)}{E} \quad (3)$$

The creep and permanent set behaviors of the rubber are combined with hyper-elasticity in a rheological model. The modelling here is composed of parallel chains with an elastic component and a viscous component apart from one chain which instead have a plasticity component to include permanent set. The rheological network is portrayed in Figure 1 and is in the numerical FE-implementation generalized to 3 dimensions. All elasticity (springs in Figure 1) is modelled with the same hyper-elastic model while each chain (dash-pots) has different viscous behaviors. Furthermore, the stress in each chain is scaled with an individual factor S_i (index i representing chain number) so they add with different amounts to the total response.

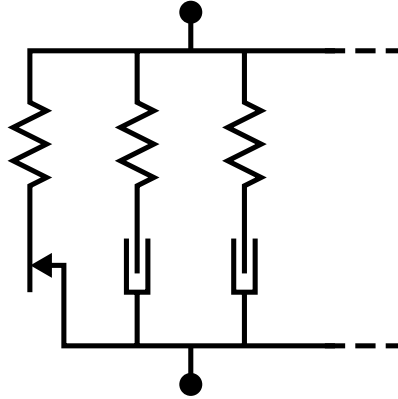


Figure 1 Rheological network with multiple chains where the springs model hyper-elasticity, dash-pots model viscoelasticity and one slider models plasticity.

The viscoelasticity behavior gives effects like creep and relaxation. The dash-pots in Figure 1 represent viscoelastic behavior given by a creep law – a differential equation governing the creep rate $\dot{\epsilon}_{cr}$ of the form

$$\dot{\epsilon}_{cr} = \frac{d\epsilon_{cr}}{dt} = f(\sigma, \epsilon, t; C) \quad (4)$$

where σ is stress, ϵ is strain, t is time and C are material parameters.

Various creep laws exist that can be used in the rheological network. One is of strain hardening type and is used in a similar application [4] and given by

$$\dot{\epsilon}_{cr} = (A\sigma_e^n [(m+1)\epsilon_{cr}]^m)^{\frac{1}{m+1}} \quad (5)$$

where A, n, m are material parameters and σ_e is the von Mises effective stress. Another creep law developed specifically for hysteresis in rubbers is the Bergstrom-Boyce model [5] which is given by

$$\dot{\epsilon}_{cr} = A(\lambda_{cr} - 1 + H)^C \sigma_e^m \quad (6)$$

where A, C, m are material parameters and λ_{cr} is a strain measure.

Temperature dependence can also be included for the creep behavior by applying Arrhenius shift factors to the creep rate. Each chain can have an individual temperature dependence.

The plasticity that gives the permanent set behavior is included with the slider as depicted in Figure 1. Various models exist for plasticity. Either a regular method for plasticity modelling with a von Mises yield surface and linear isotropic hardening or more advanced plasticity models can be used here.

2.2 Calibration and optimization

The specific behavior of material models is determined by the parameters in the model. In an engineering application, the parameters are calibrated to the materials in use. The process of calibration takes place by adjusting the parameters, so the response of the model matches a test with a material sample. When the material model is complex, advanced methods for fitting the parameters to test data are usually needed. The method for this fitting is referred to as an optimization and is typically conducted so an error measure between test data and predicted values from simulation is minimized. If the total error is $f(\mathbf{x})$ and \mathbf{x} is the set of parameters to be calibrated, then the calibration or optimization problem to find the best parameter set \mathbf{x}^* can mathematically be formulated as

$$\mathbf{x}^* = \min_{\mathbf{x}} f(\mathbf{x}) \quad (7)$$

2.2.1 Optimization methods

Optimization is often categorized in two types – global and local optimization. Global optimization attempts to find a global minimum value in the area of interest where several local minima might be present. Typical methods are genetic algorithms, grid search and simulated annealing. Local optimization finds one minimum, usually located near a start point for the search of minimum. Although local optimization methods only find one local minimum that might not be the global minimum, they have the advantage that they are faster and more accurate than global methods.

For the case of material-model calibration local optimization methods are usually the best options since the start point can be adjusted and expected to a reasonable set of parameters. Furthermore, a proper material model is not expected to have local minima. Consequently, local optimization methods are chosen here. Local optimization methods can be divided into gradient-based and gradient-free types. A short description with some theoretical background is given here. For full reference to the methods, the reader can refer to e.g. [6]

Gradient-free methods do not compute slopes and curvature of the function to be minimized. They have the advantage that they are more robust and can handle discontinuities in the function to be minimized. Examples of such methods is the Nelder-Mead method [7] that is a generalization of the linear simplex-method. It essentially constructs a multidimensional triangle called a simplex. This is then expanded, contracted or moved depending on if the algorithm estimates that the minimum is inside or outside the simplex

The gradient-based methods are based on that near a point \mathbf{x}_0 with $\mathbf{x} = \mathbf{p} + \mathbf{x}_0$

$$f(\mathbf{x}) \approx f(\mathbf{x}_0) + \nabla f(\mathbf{x}_0)^T \mathbf{p} + \frac{1}{2} \mathbf{p}^T \nabla^2 f(\mathbf{x}_0) \mathbf{p} \quad (8)$$

When $\nabla f(\mathbf{x}_0) = \mathbf{0}$, \mathbf{x}_0 is an extreme value and also a local minimum if the Hessian $\nabla^2 f(\mathbf{x}_0)$ is positive definite. From these relations the iterative process

$$\mathbf{x}_{k+1} = \mathbf{x}_k - [\nabla^2 f(\mathbf{x}_k)]^{-1} \nabla f(\mathbf{x}_k) \quad (9)$$

can be formulated to find the \mathbf{x} that minimizes $f(\mathbf{x})$. This is essentially Newton's method for non-linear systems of equations where the Hessian corresponds to the Jacobian. Therefore the method is also for optimization called Newton's method. Each iteration requires computation of the Hessian and solution of a system of linear equations. If the Hessian, which is a matrix, can be calculated analytically, this is a fast and accurate method with quadratic convergence. Typically and for the applications in this report, it is not possible to calculate the Hessian analytically. One alternative is to evaluate it numerically with finite differences. This require a

number of evaluations of $f(\mathbf{x})$ that is proportional to the square of number of variables, i.e. number of material parameters to be calibrated. When $f(\mathbf{x})$ is time consuming to compute which is the case here, this becomes too difficult. Therefore, less expensive methods that approximate the Hessian in equation (9) can be used. These methods are called quasi Newton's method. A popular method for approximating the Hessian is the BFGS method [8].

When $f(\mathbf{x})$ is a sum of squares which typically is the case in material model calibrations, Newton's method (and quasi Newton's method) can be adjusted to exploit this. The resulting method then becomes even more efficient.

All the local optimization methods described here are candidates for the material model calibration. The software Dakota [9] is here used to perform the optimization. Dakota is a free open source software that includes all the methods described here and is developed by National Technology and Engineering Solutions of Sandia.

2.2.2 Test data

Preliminary test data of relaxation type is available in [10]. The test is on circular specimens of EPDM rubber with thickness 2 mm and diameter 28 mm. The specimens are compressed by 0.50 mm. This compression is then hold and the temperature held at 140 °C while the compressive force is monitored. Two similar specimens are tested and depicted in Figure 2.

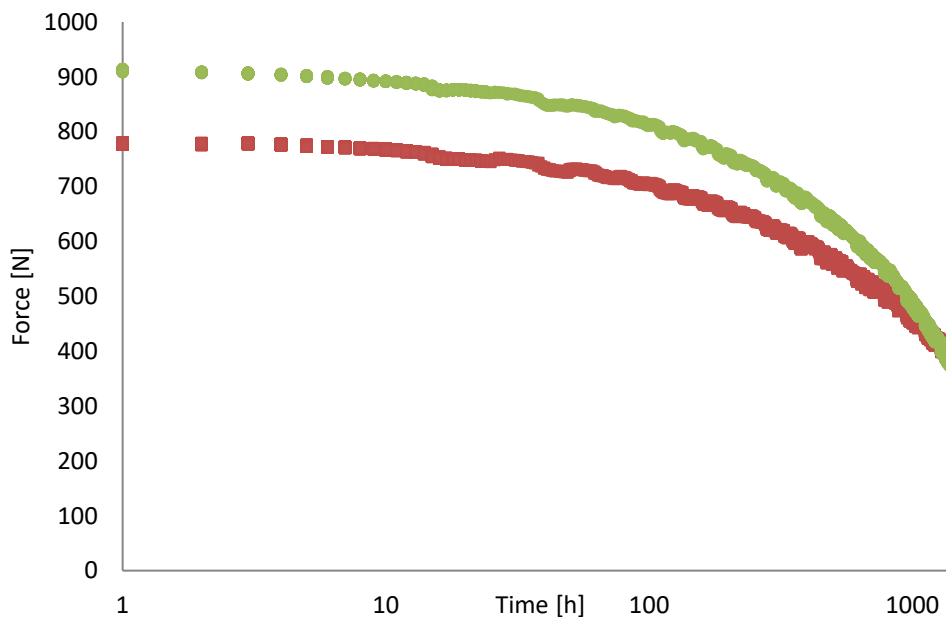


Figure 2 Relaxation test data on two specimens.

2.3 Simulation

The material-model calibration is performed for a test resembling a seal. In such a test the stress and strain in the material cannot be calculated directly. Instead, and as previously discussed, the specimen is modelled with a FE model that handles the complicated deformation. The resulting quantities, total compressive displacement and compressive force, are then available from the FE calculation and can then be compared to the experiments. The FE software package Abaqus/Standard version 2018 [11] is used for simulations.

2.3.1 Relaxation

The simulation of relaxation is performed by modelling a rubber body that is compressed between rigid planes. Since the specimens are circular, a 2D axi-symmetric geometry can be used. Symmetry is also used in the vertical z-direction in the middle of body. Hence only a 2D simulation of a quarter of the body cross section is explicitly modelled. The geometry is depicted in Figure 3.

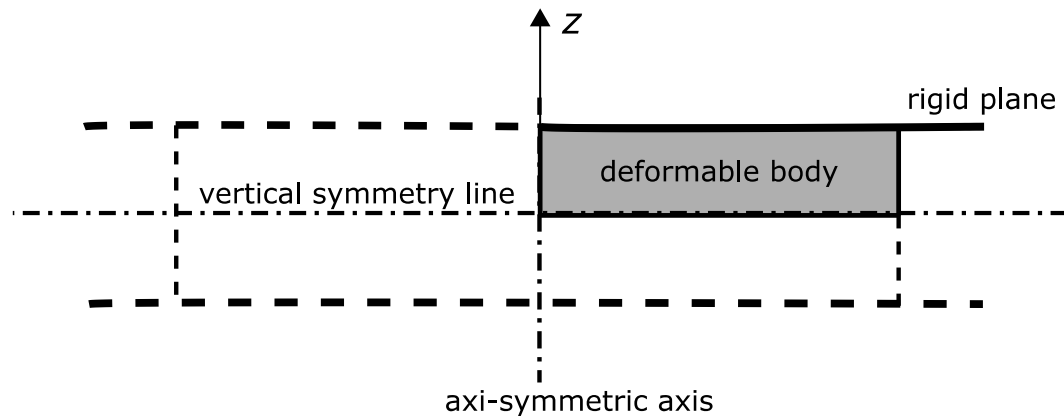


Figure 3 Geometry in the model. Dashed lines represent the boundaries of the part that are not used in the model due to symmetry. Symmetry lines and axes are represented by dash-dot lines.

The solving is performed with implicit quasi-static time integration, i.e. no inertia forces are taken into account. The elements used are linear 2D axi-symmetric elements with a hybrid formulation (Abaqus designation “CAX4RH”). Since rubber is nearly incompressible, the hybrid formulation is needed since it treats the pressure in the element as a separate degree of freedom. Without it, the pressure is un-determinate for fully incompressible materials or causing numerical difficulties for nearly incompressible materials. In Figure 4 is the FE mesh and rigid plane depicted.

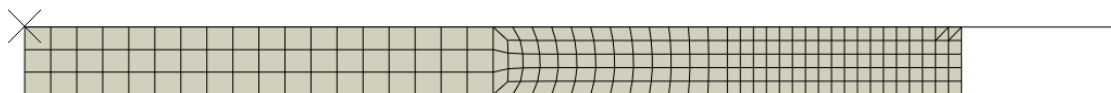


Figure 4 FE mesh and rigid plane (upper line).

The vertical symmetry is achieved by setting the vertical displacements to zero along the vertical symmetry line. The axi-symmetry is achieved by using axi-symmetric elements. The rigid plane is constrained in all degrees of freedom including rotational. The rigid plane interacts with body through contact using 0.5 as coefficient of maximum friction.

The loading takes place by forcing the rigid plane down towards the vertical symmetry line. To model the relaxation loading, the plane is in a first step moved half (to account for vertical symmetry) the distance of the total compression. Then in a second step the displacement of the rigid plane is fixed while the reaction force is monitored as resulting force to be compared to relaxation tests. In Figure 5 are FE simulation results given before relaxation starts and afterwards.

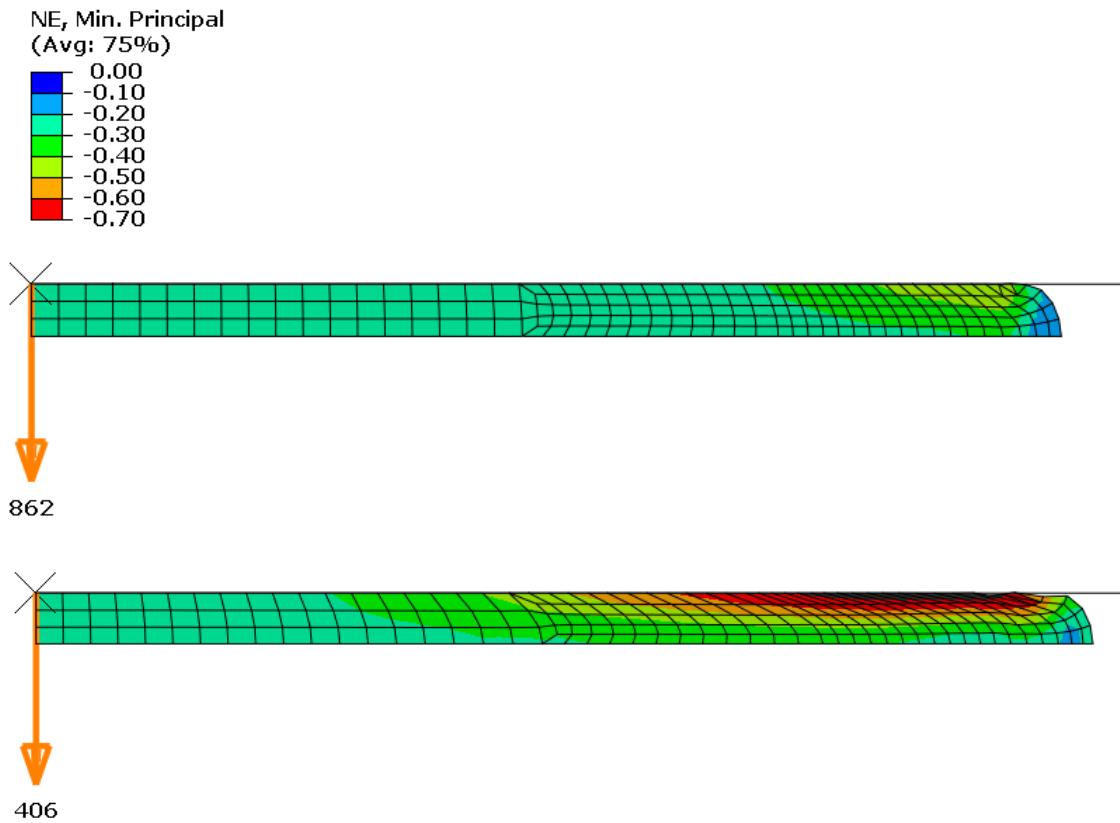


Figure 5 FE simulation results before relaxation (upper) and at end of relaxation simulation (lower). The color contour is minimum (compressive) principal strain and the arrows are the reaction force in Newtons.

2.3.2 Compressive set

Simulation of compressive set testing can be performed with same model as for relaxation by adding an un-loading step after the relaxation step. In the un-loading step, the rigid plane is released so the contact is lost. The seal will then over time expand through creep and the difference between the partially expanded deformation and original shape will be the compressive set. The time when the compressive set is determined from the simulation can either be a predetermined time corresponding to a test or sufficiently long to correspond to a permanent set.

2.3.3 Leak and tightness

Leaking and tightness of a compressed seal that are to contain a pressurized fluid can be simulated with FE modelling [4]. The modelling of an o-ring is setup with contacts similarly to what is described for the relaxation simulation. In addition a feature called pressure penetration is added. This feature adds the pressure of the contained surfaces of seal and other parts that are not in contact. If separation, then occurs for some part of the contacting surfaces the pressure is also added to these parts of the surface.

3 Results

Some first attempts for calibration of the preliminary test data presented in section 2.2.2 is given here. The rheological network model presented in section 2.1 and Figure 1 contains a chain with a spring and slider to include elasticity and plasticity respectively. The results in this report are mere of relaxation type and since the plasticity behavior is best evaluated by including compression set data, the elastic-plastic chain is not included.

The elastic parts in the rheological network have the same hyper-elastic model. Since the Neo Hookean model is used, only two parameters are needed for the elastic part. In [4] where similar simulations and calibrations were performed for EPDM rubber, Neo-Hookean parameters corresponding to Poisson's ratio 0.48 for the small strains linear elastic limit were found to be suitable. Therefore, the elastic parameters are also here chosen to similarly match Poisson's ratio 0.48. Then the elastic parameters also need to be adjusted to match the stiffness seen in the test. This can be performed simply by manually adjusting one of the material constants in the Neo-Hookean model and calculating the other to have Poisson's ratio 0.48 using equations (2) and (3) so the simulated response matches the initial measurements using the first evaluation point as described later. The resulting parameters are $C_{10} = 0.13682$ MPa and $D_1 = 0.296296$ MPa⁻¹ which correspond to Young's modulus 0.81 MPa in the small strain linear elastic limit.

Two material models are tried by performing a calibration for each of them. One material model with a single visco-elastic chain and one material model with two visco-elastic chains. The used optimization method is the least-squares variant of the quasi Newton's method described in section 2.2.1. A selection of eleven points for the least-squares evaluations is chosen logarithmically distributed with a bias towards longer time. This bias is chosen to have more points when there are more relaxation in the material. Since there are two test series, two evaluations are performed for each evaluation point. This will cause the calibration to try to find a solution in the middle of the two data sets. In Figure 6 and Figure 7 are the resulting calibrations given with the evaluation points indicated. In Figure 8 and Figure 9 are the results for the initial guess of material parameters i.e. the material model that the optimization routine starts with given. In Table 1 are the calibrated parameters given for the two material models.

Table 1 Calibrated parameters for the two rheological networks where the parameter indices represent a chain in the rheological networks.

Parameter	Single Chain	Two Chains
A_1 [MPa ^{-n₁} s ^{-m₁}]	$1.13583 \cdot 10^{-5}$	0.0263145
n_1	1.637635	3.552877
m_1	-0.089125	-0.076103
S_1	1.0	0.343194
A_2	n/a	$5.5601435 \cdot 10^{-5}$
n_2	n/a	0.333713
m_2	n/a	-0.182676
S_2	n/a	0.656806

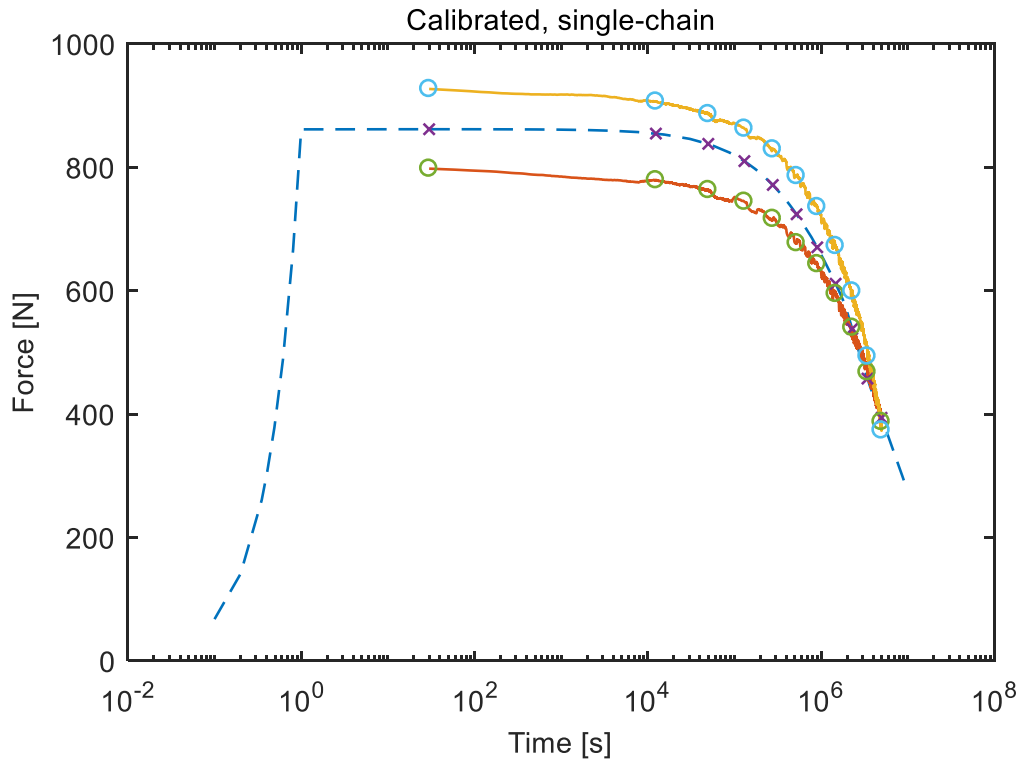


Figure 6 Relaxation forces from the tests (solid lines) and the simulation (dashed line) with the single-chain material model and calibrated material parameters. The circles are evaluation points from the testing data and the x-markers are evaluation points from the simulations.

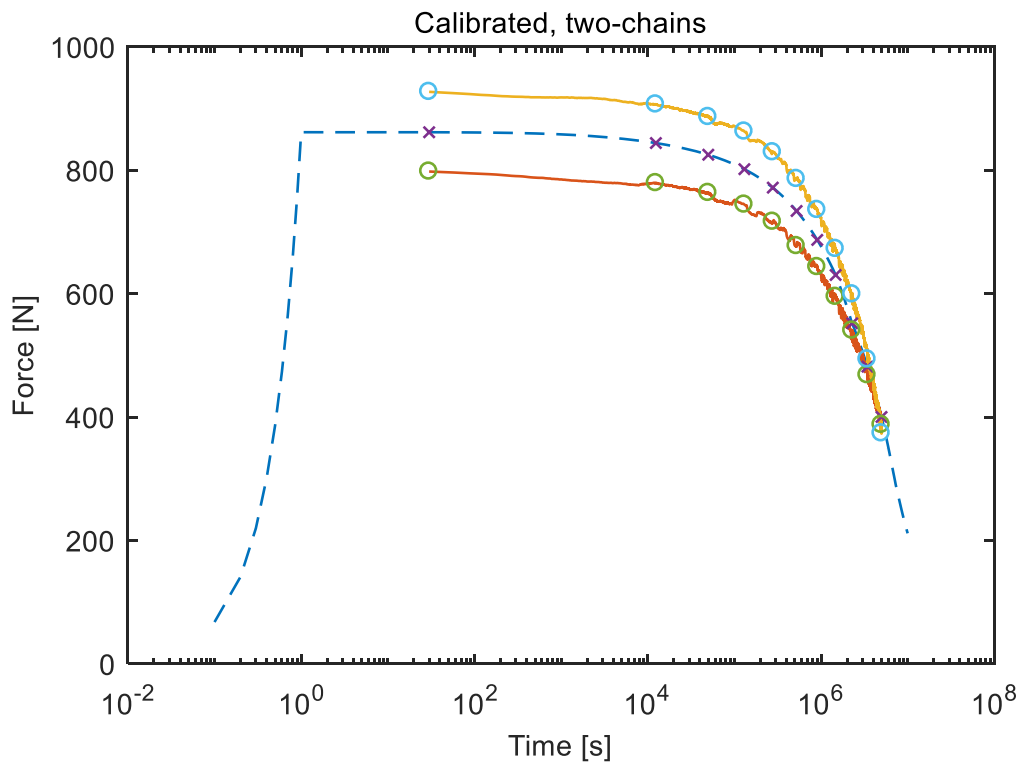


Figure 7 Relaxation forces from the tests (solid lines) and the simulation (dashed line) with the two-chains material model and calibrated material parameters. The circles are evaluation points from the testing data and the x-markers are evaluation points from the simulations.

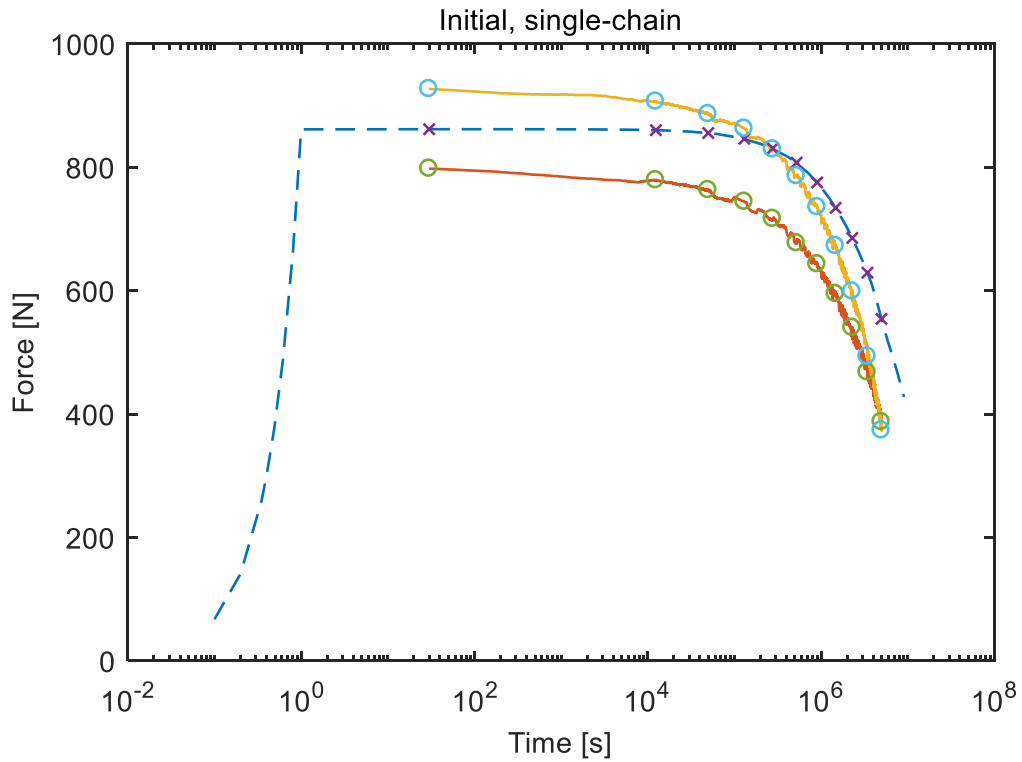


Figure 8 Relaxation forces from the tests (solid lines) and the simulation (dashed line) with the single-chain material model and initial guess for the material parameters. The circles are evaluation points from the testing data and the x-markers are evaluation points from the simulations.

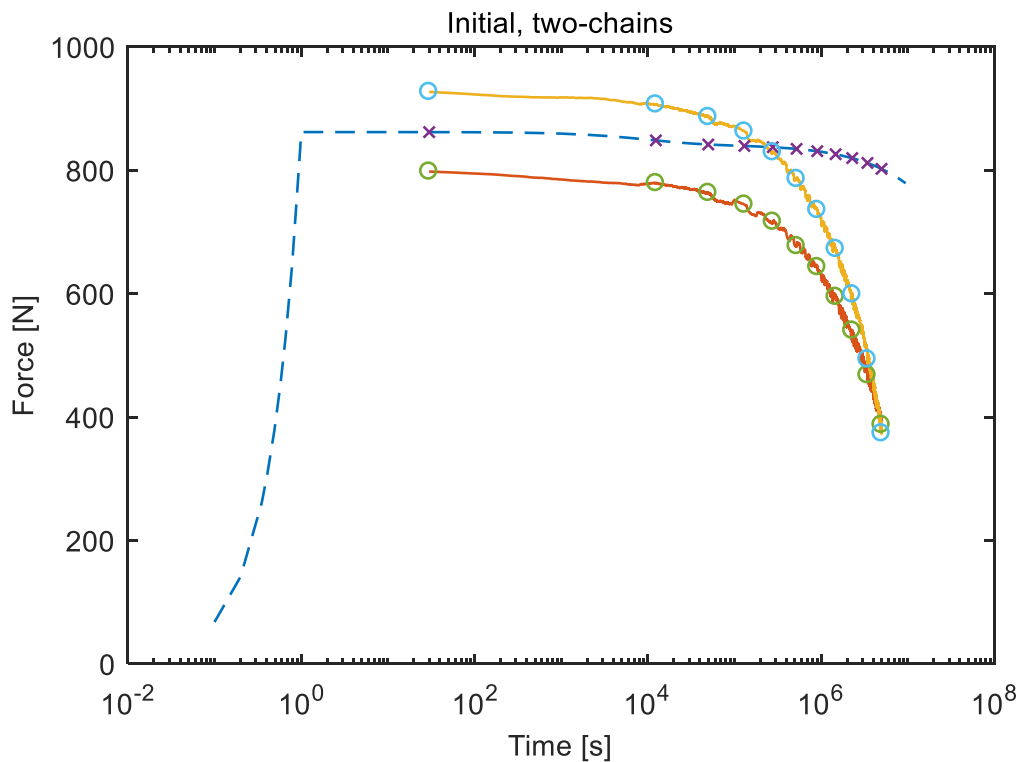


Figure 9 Relaxation forces from the tests (solid lines) and the simulation (dashed line) with the two-chains material model and initial guess for the material parameters. The circles are evaluation points from the testing data and the x-markers are evaluation points from the simulations.

When comparing the single-chain and two chains material model it is seen that the two-chains material model matches the test data slightly better than the single-chain material model. The two-chains material model both matches the initial behavior with some slope, is nearer the middle of the two data sets and with better matching at longer time durations. A possible physical interpretation of the two-chains material model is that there are two molecular mechanisms in the material causing creep behavior. One mechanism that acts on short timescales in the order of 10^4 seconds. The other acts on long timescales between 10^4 and 10^7 seconds.

If the better performance of the two-chains material model over the single-chain material model is worth the added complexity and several accompanying material parameters can be discussed. For application of seals, the long-term relaxation is of most interest. The single-chain material model might therefore be adequate if the test data for longer times can be predicted. Furthermore, when more material features like plasticity and temperature dependency are also included, the extra complexity and parameters might be too challenging for the two chains model.

4 Conclusions and further work

It is shown how the relaxation tests can be used together with simulations to calibrate rubber material behavior. When comparing the simulated responses to test data, the agreement seems to be good since the simulated response falls very near the middle of the two test series where the optimization routines are expected to find a solution when they are successful and accurate.

The difference between the two test series can be seen as an indication of the magnitude in the measurement uncertainty and scatter in the material behavior variation. To better quantify the variation, more tests are needed. However, for a real application, more accuracy than the variation is of limited use but serves a purpose in this context to assess the capabilities of the modelling.

The results here are on the preliminary relaxation tests. As more tests get available in the project, more features in the material model as described in section 2.1 will be added to the modeling. Calibration attempts will then be performed to assess both if calibration is possible and if the chosen material models are suitable. Material model features to add are plasticity to include permanent set and temperature dependence with Arrhenius shift factors. The Arrhenius shift factors can be used to predict the relaxation at other temperature levels. Different options are possible to set the Arrhenius activation energy parameter. Either it is also calibrated from relaxation tests with different temperatures. Or it is determined with some other type of testing and then validated with comparison of relaxation tests with different temperatures. It should also be investigated if radiation levels can be treated in a similar way.

In this report, the test specimens are of flat shape. Test data on o-ring samples will be better as this is closer to reality and a more complex stress-strain state can develop in a compressed o-ring compared to compression of flat specimens. Simulation of leakage and tightness can then be performed with the pressure penetration method.

Actions that are possible to perform in future work are:

- Calibration on more test data and different materials
- Plasticity material modelling that can be used to evaluate compressive set testing
- Temperature dependence with Arrhenius shift factors
- Leak and tightness simulations

5 Acknowledgements

This work is part of the COMRADE project in SAFIR2018 research programme. The Finnish State Nuclear Waste Management Fund (VYR) and Swedish Radiation Safety Authority are acknowledged for funding this work.

6 References

- [1] M. Granlund och A. Jansson, "WP1 COMRADE - Development of condition monitoring methods for polymeric components including low dose rate radiation exposure," SP Technical Research Institute of Sweden, Borås, 2017.
- [2] P.-E. Austrell, "MODELING OF ELASTICITY AND DAMPING FOR FILLED ELASTOMERS," Lund University, Lund, 1997.
- [3] P. K. Freakley och A. Payne, Theory and Practice of Engineering with Rubber, Applied Science Publishers, 1978.
- [4] J. H. Sällström, J. Sandström och S.-E. Sällberg, "Täthet hos flänsförband mellan stora polyetenrör och ventiler – experimentell och numerisk studie," Svenskt Vatten Utveckling, Bromma, 2016.
- [5] J. Bergström och M. Boyce, "Constitutive modeling of the large strain time-dependent behavior of elastomers," *Journal of the Mechanics and Physics of Solids*, vol. 46, nr 5, pp. 931-954, 1998.
- [6] S. Nash och A. Sofer, Linear and Nonlinear Programming, McGraw-Hill, 1996.
- [7] J. Nelder och R. Mead, "A Simplex Method for Function Minimization," *The Computer Journal*, vol. 7, nr 4, p. 308–313, 1965.
- [8] R. Fletcher, "A new approach to variable metric algorithms," *The Computer Journal*, vol. 13, pp. 317-322, 01 01 1970.
- [9] B. Adams, L. Bauman, W. Bohnhoff, K. Dalbey, M. Ebeida, . J. Eddy, M. Eldred, P. Hough, K. Hu, J. Jakeman, J. Stephens, L. Swiler, D. Vigil och T. Wildey, "Dakota, A Multilevel Parallel Object-Oriented Framework for Design Optimization, Parameter Estimation, Uncertainty Quantification, and Sensitivity Analysis: Version 6.0 User's Manual," University of California, California, 2017.
- [10] E. Bernmalm Törnström, "Lifetime criteria of EPDM O-ring seals in nuclear power plants," Chalmers University of Technology, Göteborg, 2017.
- [11] Dassault Systèmes, *Abaqus 2018 Documentation*, 2018.

RISE Research Institutes of Sweden AB
Safety - Mechanics Research

Performed by

Examined by



Signed by: Johan Sandström
Reason: I am the author of this document
Date & Time: 2018-03-20 17:31:15 +01:00

Johan Sandström



Erland Johnson